



ISTITUTO NAZIONALE DI RICERCA METROLOGICA Repository Istituzionale

Validation of phosphor thermometry for industrial surface temperature measurements

Original

Validation of phosphor thermometry for industrial surface temperature measurements / Rosso, Lucia; Tabandeh, Shahin; Beltramino, Giulio; Fericola, Vito. - In: MEASUREMENT SCIENCE & TECHNOLOGY. - ISSN 0957-0233. - 31:3(2020), p. 034002. [10.1088/1361-6501/ab4b6b]

Availability:

This version is available at: 11696/61705 since: 2021-04-20T16:16:41Z

Publisher:

IOP

Published

DOI:10.1088/1361-6501/ab4b6b

Terms of use:

This article is made available under terms and conditions as specified in the corresponding bibliographic description in the repository

Publisher copyright

(Article begins on next page)

PAPER • OPEN ACCESS

Validation of phosphor thermometry for industrial surface temperature measurements

To cite this article: Lucia Rosso *et al* 2020 *Meas. Sci. Technol.* **31** 034002

View the [article online](#) for updates and enhancements.

Validation of phosphor thermometry for industrial surface temperature measurements

Lucia Rosso¹, Shahin Tabandeh, Giulio Beltramino¹ and Vito Fericola

Istituto Nazionale di Ricerca Metrologica (INRIM), Strada delle Cacce 91, Torino, Italy

E-mail: l.rosso@inrim.it

Received 4 July 2019, revised 20 September 2019

Accepted for publication 7 October 2019

Published 2 December 2019



Abstract

Surface temperature measurements are required by the aerospace and automotive industries to guarantee high-quality products and optimize production processes. Accurate and reliable measurement of surface temperature is very challenging in an industrial environment. Surface contact probes are widely used but poorly characterized, while non-contact infrared thermometry is severely hampered by the unknown emissivity of the surface and by problems caused by stray radiation from the background. An alternative approach to the above techniques is phosphor thermometry, used here in a hybrid contact/non-contact approach.

In this work, the development of a lifetime-based phosphor thermometer, its application to industrial surface temperature measurement and its validation are reported in a metrologically sound manner. The phosphor thermometer was initially calibrated by contact on a reference calibrator system at the Istituto Nazionale di Ricerca Metrologica to provide SI traceability to the measurements at the industrial level; the system was later validated by exploiting a metal phase-change method. The robustness of the approach against a strong radiative background was also investigated. A comprehensive uncertainty analysis was carried out, resulting in an expanded uncertainty ($k = 2$) lower than 1.4 °C over the temperature range from the ambient to 450 °C.

The phosphor-based thermometer was then tested at industrial manufacturing premises to measure the surface temperature of aluminium alloy billets during the pre-heating phase before forging. The phosphor-based approach was compared with radiation and contact thermometry in both static and dynamic measurement conditions. The experimental results proved that phosphor thermometry, besides being a valid alternative to conventional techniques, may offer better performance in an industrial setting.

Keywords: phosphor thermometry, surface temperature, industrial manufacturing, material heat treatment, phosphorescence lifetime

(Some figures may appear in colour only in the online journal)

1. Introduction

A wide range of applications in the aerospace and automotive industries rely on accurate surface temperature measurements

¹ Author to whom any correspondence should be addressed.



Original content from this work may be used under the terms of the [Creative Commons Attribution 3.0 licence](https://creativecommons.org/licenses/by/3.0/). Any further distribution of this work must maintain attribution to the author(s) and the title of the work, journal citation and DOI.

to ensure high efficiency in the manufacturing process and favourable quality of the final product. For example, in heat treatment of aluminium alloy for the hot forming and forging of mechanical components, control of the temperature at the billet pre-heating stage (within ± 5 °C) is critical. Surface temperature measurements by contact thermometry are often used but have many weaknesses and shortcomings; in fact, it is necessary to maximize the thermal contact between the probe and the surface and, at the same time, minimize the

thermal heat flux along the sensor probe, so that the surface temperature is not significantly perturbed.

To some extent, infrared (IR) thermometry, as a non-contact technique, may overcome the above-mentioned limitation. However, other difficulties need to be addressed, including the unknown and often process-dependent emissivity of the surface as well as the presence of stray radiation from adjacent sources, which may end up giving reading errors of tens of degrees.

Temperature-sensitive coatings for surface temperature measurements are also available. Temperature-sensitive paints are generally limited to temperatures lower than 200 °C while thermal paints are not suitable for time-resolved measurements and can give only a rough estimate of the peak temperature corresponding to the irreversible colour change of the paint [1, 2].

An alternative to the approaches outlined above, which may also overcome some of the problems encountered with traditional methods, is phosphor thermometry. This is a robust hybrid method (i.e. contact/non-contact) to remotely determine the temperature of a surface, independent of surface emissivity and less sensitive to background radiation than IR thermometry. This method has been used in remote measurements of the temperature of both static and moving surfaces even in hostile high-temperature environments, such as in the presence of vibrations, flame, high pressure and electromagnetic interference [3, 4]. In these applications, to minimize the effects of the intense thermal radiation background typical of high-temperature measurements, the best choice is to use phosphors that emit in the blue spectral region where blackbody radiation is low [5, 6]. The application of phosphor thermometry is very wide in fields other than aerospace, and ranges from automotive to the naval and energy fields and solid-state light sources [7–11].

Currently the temperature range for application of phosphor thermometry extends from cryogenic temperatures up to almost 2000 K [12, 13]. A thin film of a thermographic phosphor can be coated or sprayed on the surface under test (contact) and interrogated optically (non-contact). The luminescence emitted by the phosphor is temperature dependent and can be exploited as the temperature-sensing property. Various luminescence characteristics of phosphors are affected by temperature and may thus be exploited for temperature measurements; in the last decades, luminescence lifetime as well as the intensity ratio of different lines in the emission spectra have been the most popular approaches [14].

Comprehensive reviews of phosphor thermometry, focusing on both the key features and the application issues are available: a well-known review was published by Allison and Gillies [15], more recently Khalid and Kontis [16], Chamber and Clarke [17], Alden *et al* [18], Brubach *et al* [19] and Yi and Kim [20] surveyed and reviewed the latest advances and applications.

The present work focuses on the metrological validation of lifetime-based phosphor thermometry for industrial surface temperature measurements. With this aim, a portable fibre-optic phosphor thermometer was designed and constructed at the Istituto Nazionale di Ricerca Metrologica (INRIM). Manganese-doped magnesium fluorogermanate ($\text{Mg}_4\text{FGeO}_6\text{:Mn}$) was selected as a temperature-sensing phosphor targeted to cover

the range from ambient to 450 °C, and was calibrated by comparison against a reference surface temperature calibrator. The performance of the fibre-optic thermometer system was carefully assessed and the calibration uncertainty estimated. The phosphor-based surface temperature measurement technique was further validated using a metal phase transition method based on an ITS-90 temperature fixed point and its robustness investigated in the presence of a background of strong IR radiation. Subsequently, a rigorous analysis of the measurement uncertainty of the field application was performed.

The application of the thermometer system to surface temperature measurements of aluminium alloy billets during pre-heating treatment at industrial manufacturing premises is presented, as well as *in situ* validation by comparison against two conventional techniques, contact thermometry and radiation thermometry.

2. Implementation of the phosphor thermometer

2.1. Principle

The operating principle of the phosphor thermometer developed at INRIM is based on measurement of the lifetime of a thin layer of a temperature-sensitive phosphor coated on the surface under test. By irradiating such a phosphor with a light pulse and then observing the subsequent decay in the intensity, the temperature-dependent phosphorescence lifetime can be determined. In most cases, the phosphorescence decay process can be described through a single exponential as follows:

$$I = I_0 \exp(-t/\tau) + b \quad (1)$$

where I_0 is the initial intensity of the phosphorescence light, t is the time, τ is the decay time constant of the signal (i.e. the phosphorescence lifetime of the phosphor) and represents the time needed for intensity to reduce its value by a factor of e^{-1} and b is a baseline offset which incorporates electronics offset and radiative background. The time constant τ can be determined from the least-squares fit of equation (1) to the measurement data [21] and may then be used as a measure of the phosphorescence lifetime. The phosphorescence lifetime of a phosphor decreases with increasing temperature. Optical excitation of a phosphor by a suitable light signal brings electrons into excited states; the subsequent return to the ground state may occur through both radiative and non-radiative (phonon quenching) processes. Such processes have different probabilities of occurrence (i.e. different decay rates) and compete with one another. The decay time τ of the emission is determined by the rates of both decay processes, radiative and non-radiative (actually, the rate of non-radiative processes is a function of temperature and this explains the temperature dependence of the decay time). Once the phosphor has been calibrated over the temperature range of interest, the temperature can be retrieved by the measurement of its phosphorescence lifetime.

2.2. Experimental setup

Several phosphors were considered for this application in hybrid (contact/non-contact) thermometry over the

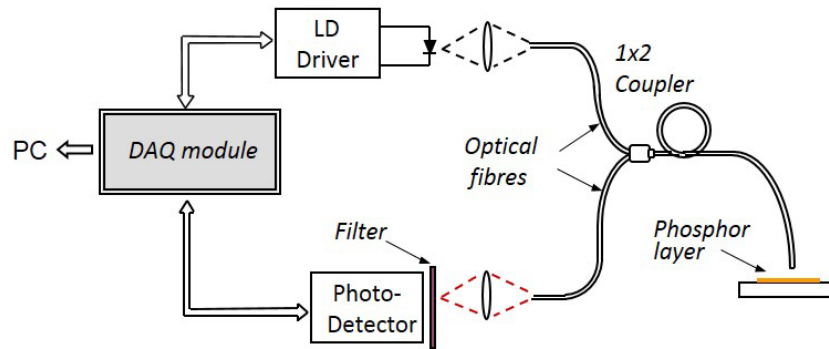


Figure 1. Schematic of the phosphor-based fibre-optic thermometer.

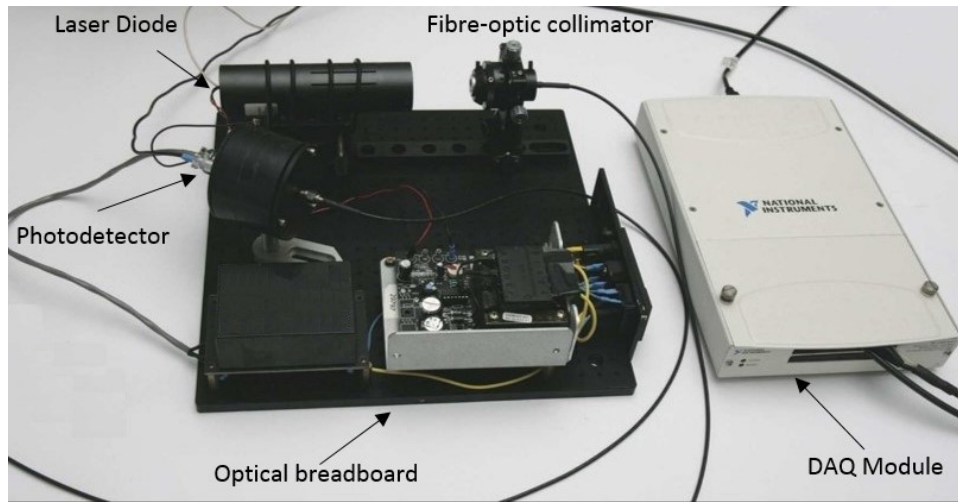


Figure 2. The portable phosphorescence excitation/detection unit.

temperature range from ambient to 500 °C. Magnesium fluorogermanate doped with manganese ($\text{Mg}_4\text{FGeO}_6\text{:Mn}$) was eventually selected. It exhibits a wide operating range, from cryogenic temperatures [12] to about 1000 K [22], and a satisfactory temperature sensitivity over the whole range. In recent decades it has been used in several phosphor thermometry applications [23–26]. A suitable high-temperature ceramic binder was chosen in order to obtain a robust, optically transparent and thin surface coating. The phosphorescence emission of $\text{Mg}_4\text{FGeO}_6\text{:Mn}$, which occurs in the red spectral region ($\lambda = 620\text{--}700\text{ nm}$), results from strong absorption of light with peaks at about 300 nm and 420 nm. Efficient optical pumping was achieved with excitation at 405 nm with a laser diode (LD). This LD emission was modulated in the form of repetitive rectangular pulse, with a period set to be roughly ten times bigger than the expected decay time, and a duty cycle of 50%, collimated into one branch of a 1×2 fibre coupler and delivered to the phosphor sensing layer. The second branch of the fibre coupler was used to guide out the phosphorescence response to a detection stage. Here, a silicon p-i-n photodiode converted the optical signal into an electrical signal which was then sampled at a frequency of 1 MHz and converted by a 16-bit DAQ module (NI DAQ model 6251), interfaced to a PC, for further processing. The temperature-dependent phosphorescence lifetime was then converted into

a temperature through a pre-set calibration curve of the sensor, as investigated in a separate experiment. A schematic diagram of the fibre-optic thermometer is shown in figure 1.

In view of its industrial use, the thermometer system was constructed in a compact and portable unit. Phosphorescence excitation/detection devices with the associated optics were assembled on a small optical breadboard (300 mm \times 300 mm) directly connected to an optical fibre and to an external DAQ module to convert the phosphorescence decay time into a temperature reading (figure 2). The overall cost of such an experimental setup does not exceed €10 000.

2.3. Data processing and evaluation

For the evaluation of temperature-dependent decay time τ , the response of the phosphor to a pulsed light excitation signal was acquired by sampling the transient decay curve in a given time window, after the excitation light had ceased. The time window interval corresponds to a multiple of the decay time constant to be estimated [21]. The phosphorescence signal, which to a first approximation can be modelled by a single exponential decay as reported in equation (1), was processed in the frequency domain by means of its Fourier transform $F(\omega)$:

$$F(\omega) = \Im [A \exp(-t/\tau) + B] \quad (2)$$

resulting in

$$F(\omega) = \frac{A}{1/\tau - j\omega} + B\delta(\omega) \quad (3)$$

where $\delta(\omega)$ is the Dirac function. Thus, for any non-zero angular frequency ω , the decay time τ can be calculated as the ratio of the imaginary to the real part of $F(\omega)$ through the relation

$$\tau = \frac{\text{Im}[F(\omega)]}{\omega \text{Re}[F(\omega)]}. \quad (4)$$

For an N -point fast Fourier transform (FFT), to take into account the discrete sampling effect in order to estimate the ‘unbiased’ phosphorescence decay time, equation (4) becomes [21]

$$\tau = \left[\frac{1}{\Delta t} \ln \left(\frac{\text{Re}[\text{FFT}(\omega)]}{\text{Im}[\text{FFT}(\omega)]} \cdot \sin(\omega_i \Delta t) + \cos(\omega_i \Delta t) \right) \right]^{-1} \quad (5)$$

where Δt is the sampling interval and the angular frequencies ω_i are given by

$$\omega_i = \frac{2\pi \cdot i}{N \cdot \Delta t} \quad \text{for } i = 1, 2, \dots, N-1. \quad (6)$$

The decay time τ can be evaluated from equation (5) for each discrete frequency ω_i . In practice, τ is only estimated for the first harmonic, since it has a higher amplitude respect to the others and consequently a higher signal-to-noise ratio.

2.4. Phosphor calibration

Before its use, the phosphor was calibrated by comparison against a suitable, SI-traceable, temperature standard. Actually, to ensure that the calibration conditions were as close as possible to the actual operating conditions, the phosphor was calibrated by contact with the INRIM reference surface calibration system in the temperature interval from 50 °C to 450 °C. This system is based on a temperature-controlled block, whose surface acts as the temperature reference. The aluminium block is mounted on a flat round heater and is surrounded by thermal insulators. Three calibrated platinum resistance thermometers (PRTs), which are radially inserted at different depths, enable the measurement of the temperature profile along the vertical axis. The temperature of the reference surface is estimated by linear extrapolation of the temperature readouts given by two PRTs, while the third thermometer is used to check the linearity of the temperature profile across the block.

The phosphor was mixed with a high-temperature binder (Aremco Ceramabind 643-2) in a 1:5 ratio by weight and brush-coated on the surface of the aluminium block. To ensure good adhesion of the coating, the block was kept at room temperature for 24 h and then at 100 °C for 1 h, at 250 °C for 2 h and finally brought to the maximum temperature of interest, 450 °C, with a heating rate of 2 °C min⁻¹ and maintained at this temperature for at least 1 h. The thickness of the coating was about 75 µm. A 3 m long bundle of multi-mode optical fibres (with numerical aperture of 0.22, a total light collecting area of about 1 mm² and a signal attenuation lower than

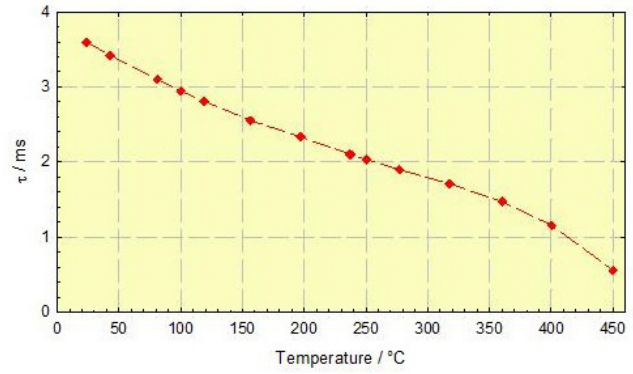


Figure 3. Calibration curve of Mg₄FGeO₆:Mn. The phosphorescence lifetime versus reference surface temperature generated by the aluminium calibrator block.

10 dB km⁻¹), placed at a distance of about 5 mm from the surface, was used for the phosphor excitation and for collecting its luminescent response. At each surface temperature generated on the reference block, the corresponding phosphorescence lifetime (τ) was recorded. The calibration results, reported in figure 3, show a monotonic behaviour, in good agreement with the data available in the literature [22]. The temperature sensitivity of the sensor varies from 6 µs °C⁻¹ to a maximum of about 10 µs °C⁻¹ over the whole temperature range.

An uncertainty analysis for the phosphor calibration on the surface reference block was also performed at several temperatures in the range of interest, and the results are reported in Table 1. Following [27], the calibration standard uncertainty, u_{Cal} , was calculated at each temperature by combining quadratically the input uncertainty contributions, i.e. taking the square root of the sum of the squares of the individual uncertainties. The input quantities are assumed to be uncorrelated.

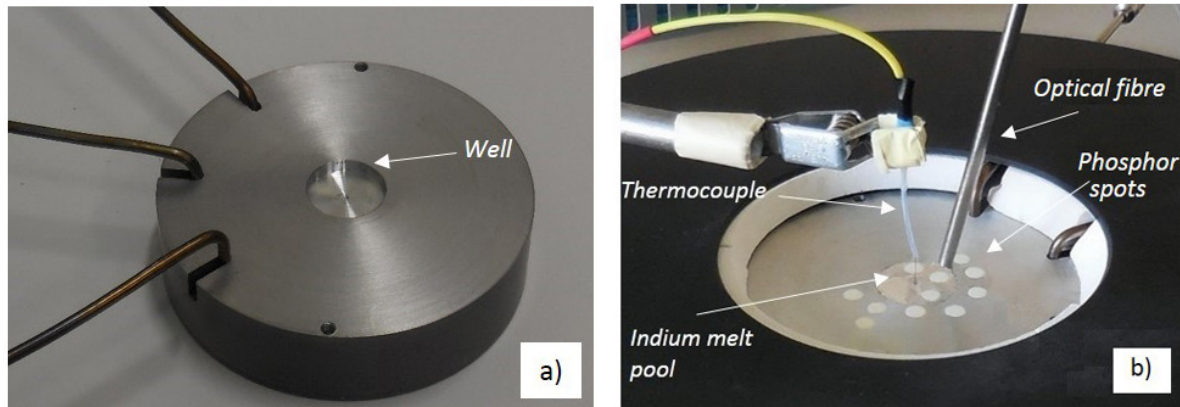
The major sources of uncertainty which have been taken into account are the uncertainty of the reference surface temperature and the repeatability of the lifetime. The first contribution comes from the propagation of the uncertainty of the individual PRTs through the linear extrapolation model and the second term considers the stability of the surface temperature as well as different sources of electrical and optical noise. The uncertainty of the exponential fitting and the data acquisition uncertainty make minor contributions. The first considers the goodness of fit through the deviation of acquired data points from their final fitting and the latter accounts for the propagation of acquisition uncertainties through the mathematical model. Among the sources of uncertainty considered, the most significant contribution is due to the repeatability of the estimated lifetime, and the smallest one typically comes from the exponential fitting. The last term is evaluated by exploiting the Monte Carlo simulations considering 2×10^6 sets of randomly generated data points according to the input Gaussian probability density functions.

2.5. Validation of the phosphor-based technique

Once calibrated, the phosphor-based system was further validated by measuring the phase transition temperature of a pure

Table 1. Uncertainty analysis of $\text{Mg}_4\text{FGeO}_6\text{:Mn}$ calibration on the aluminium block at several temperatures T .

Input uncertainty component	$T = 50\text{ }^\circ\text{C}$	$T = 100\text{ }^\circ\text{C}$	$T = 200\text{ }^\circ\text{C}$	$T = 300\text{ }^\circ\text{C}$	$T = 400\text{ }^\circ\text{C}$
Uncertainty of the reference surface temperature	0.09 $^\circ\text{C}$	0.11 $^\circ\text{C}$	0.14 $^\circ\text{C}$	0.16 $^\circ\text{C}$	0.19 $^\circ\text{C}$
Repeatability of the lifetime estimate	0.127 $^\circ\text{C}$	0.164 $^\circ\text{C}$	0.192 $^\circ\text{C}$	0.236 $^\circ\text{C}$	0.277 $^\circ\text{C}$
Uncertainty of the exponential fitting	0.002 $^\circ\text{C}$	0.003 $^\circ\text{C}$	0.003 $^\circ\text{C}$	0.003 $^\circ\text{C}$	0.002 $^\circ\text{C}$
Data acquisition, sampling effects	0.010 $^\circ\text{C}$	0.013 $^\circ\text{C}$	0.015 $^\circ\text{C}$	0.017 $^\circ\text{C}$	0.01 $^\circ\text{C}$
Calibration standard uncertainty, u_{Cal}	0.16 $^\circ\text{C}$	0.20 $^\circ\text{C}$	0.24 $^\circ\text{C}$	0.29 $^\circ\text{C}$	0.34 $^\circ\text{C}$

**Figure 4.** (a) The reference block showing the shallow well used to house the indium. (b) Arrangement for the measurement of phosphor temperature at the indium melting temperature.

metal. Initially a shallow depression (diameter 20 mm, depth 3 mm) was machined on the reference surface block and filled with a small amount (about 8 g) of high-purity (99.999%) indium (see figure 4(a)). The freezing point temperature of indium (156.5985 $^\circ\text{C}$) is a defining fixed point of the International Temperature Scale of 1990 (ITS-90), while its melting point temperature differs by a few tenths of a mK from that of freezing [28]. The realization of a melting plateau is easier than that of a freezing plateau because there are no problems with supercooling and induction of nucleation; furthermore, the duration of the melting plateau can be longer than that of the freezing plateau. For these reasons, in the present work, the indium melting point was chosen for validation of the phosphor-based technique. Thus, a small spot of phosphor was placed on the indium layer and its phosphorescence decay time was measured by means of the fibre-optic thermometer (figure 1) during the indium melting phase. Several tests were performed to identify the best way to ensure a reproducible phase change. A junction of a 100 μm type-T thermocouple, inserted into the melting pool, was also used to check the starting point of the plateau (figure 4(b)). Eventually, an indium melting plateau lasting more than 30 s was obtained.

The phosphor response at the indium melting temperature, as converted to temperature through the phosphor calibration curve, is depicted in figure 5. Repeated melting cycles were performed, and for each cycle the differences between the temperatures measured by the phosphor and the nominal temperature of the melting point (used as reference) were measured. The corresponding results are shown in figure 6, with the error bars representing the expanded measurement uncertainty with a coverage factor $k = 2$, which corresponds to a coverage interval of about 95% [27]. A maximum

difference of about 0.3 $^\circ\text{C}$, i.e. less than the associated measurement uncertainty, was obtained, thus indicating that the phosphor-based technique was successfully validated for surface temperature measurements on metal surfaces.

2.6. Effect of IR background radiation

The potential use of the phosphor-based technique for surface temperature measurements in industrial applications needs to be investigated in conditions where the presence of high-temperature furnaces produces strong IR background radiation. In particular, with regards to the targeted process (i.e. thermal processing of aluminium alloy billets before forging), IR background radiation is expected to be of the order of several kW m^{-2} . In the actual implementation of the fibre-optic thermometer in this industrial application, by taking into account the numerical aperture of the multimode optical fibres and the low emissivity of the aluminium billet ($\varepsilon \sim 0.2$), the detected background radiation is significantly lower.

In order to assess its impact on measurement accuracy, an IR lamp was used to generate background radiation of about 1 kW m^{-2} (locally measured by a pyranometer) on the reference block for surface temperature, coated with a small spot of phosphor. The IR lamp was modulated through an on/off signal, and in the meantime the phosphor response was recorded. Phosphor measurements indicate a slight temperature drift due to surface warming by IR radiation of approximately 0.5 $^\circ\text{C}$ (see figure 7) in about 10–15 min. The short-term radiative disturbance of the detection system by the lamp was also investigated by measuring the instantaneous variation of the phosphorescence response when the lamp was switched on/off. A deviation of about 0.1 $^\circ\text{C}$, i.e. lower than the actual measurement repeatability (see table 1), was observed. Thus,

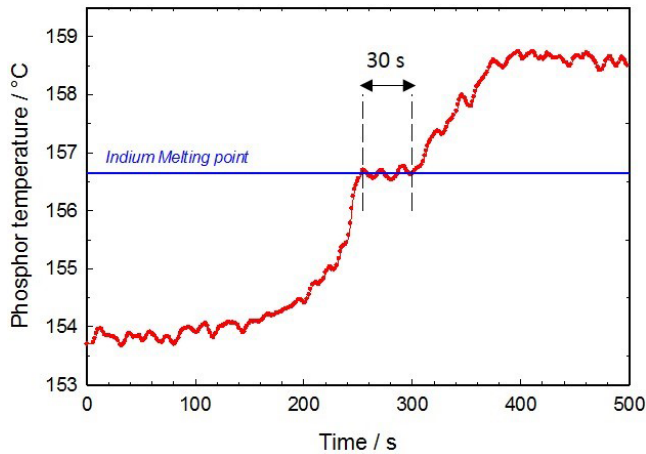


Figure 5. Phosphor response during indium melting experiment (red line).

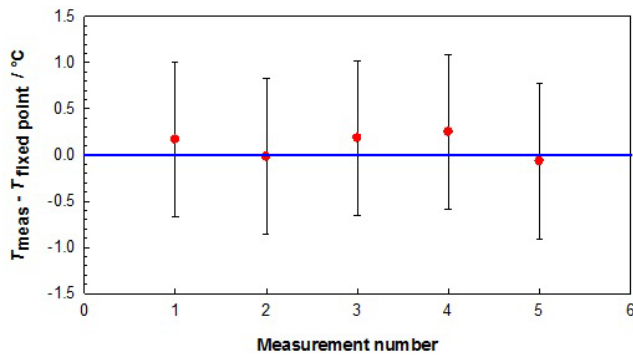


Figure 6. Differences between the temperatures measured by the phosphor and the temperature of the indium melting point (used as reference).

it can be concluded that the phosphor-based thermometer is ‘robust’ enough not to be adversely affected by a strong radiative background in industrial settings.

2.7. Measurement uncertainty in field applications

When the phosphor-based technique is employed in the field for surface temperature measurements, several contributions to uncertainty must be considered. A comprehensive evaluation of measurement uncertainty was carried out, resulting in an expanded uncertainty U (with $k = 2$) that varies from 0.6 °C at room temperature to less than 1.4 °C at 450 °C. An example of an uncertainty budget is reported in table 2 for a temperature measurement of approximately 400 °C. The standard uncertainty, u , was calculated as the square root of the sum of the squares of the individual uncertainties [27]. The table highlights that one of the major sources of uncertainty, besides the lifetime repeatability and the phosphor calibration (described in section 2.3 and reported in table 1) is due to the reproducibility of the phosphor coating method.

Actually, the main challenge in our phosphor thermometry application is to produce a consistent, robust and reproducible phosphor layer with good adhesion to the surface under test and a low, repeatable, contact thermal resistance. Although the brush-coating technique has been refined, by defining a

suitable mixing ratio of phosphor/binder, an ideal thickness of the coating and the curing process, the actual coating reproducibility nevertheless represents a significant contribution to uncertainty and must be taken into account. This contribution has been experimentally estimated by coating a two-dimensional array of phosphor spots on a uniform-temperature reference calibration surface and then measuring the phosphorescence lifetime corresponding to the different spots. The spread of the temperatures measured by the spot sensors was within 0.5 °C for both aluminium and stainless steel blocks over the whole temperature range of interest.

3. Industrial application of the phosphor-based thermometer

We now present the application of the phosphor-based technique in surface temperature measurements at an industrial manufacturing facility.

In the thermal processing of aluminium alloy billets for the moulding of mechanical components, temperature control within ± 5 °C is required during the pre-heating phase. In order to tune the process, a series of surface temperature measurements of aluminium billets were performed at the manufacturing premises of Gamma Forgiati (an Italian company operating in the forging of light metal alloy) by using an industrial furnace which reproduced the conditions present in the in-line manufacturing process in a more controlled environment. The phosphor-based approach was used and, at the same time, compared with conventional techniques, i.e. contact thermometry and radiation thermometry. Such measurements were first performed in stationary conditions (i.e. the billet was stationary inside the furnace) and subsequently in dynamic conditions (i.e. during extraction of the billet from the furnace), which better represents the actual operating conditions during the manufacturing process.

For the implementation of contact thermometry, the temperature chain used for contact temperature measurements consisted of a commercial temperature indicator with a type-K thermocouple having a 5 m stainless steel sheath. The temperature chain was calibrated for comparison in a thermostatic bath in the range from 300 °C to 500 °C, with an expanded uncertainty ($k = 2$) of about 0.9 °C.

For radiation thermometry, a Williamson multi-wavelength radiation thermometer (model Pro MW-20-20-C) was used to perform non-contact measurements. This thermometer operates at three wavelengths (1.5, 2.0 and 2.5 μm) and was calibrated by the manufacturer in the temperature range from 200 °C to 600 °C with an expanded uncertainty of 2 °C. According to the manufacturer, by using a built-in data-processing algorithm the instrument is able to accurately measure the temperature of surfaces that have low or variable emissivity.

3.1. Measurements in stationary conditions

An aluminium billet (a cylinder of diameter 28 mm and length 70 mm) was equipped with a type-K thermocouple, introduced from the back, and a series of phosphor spots

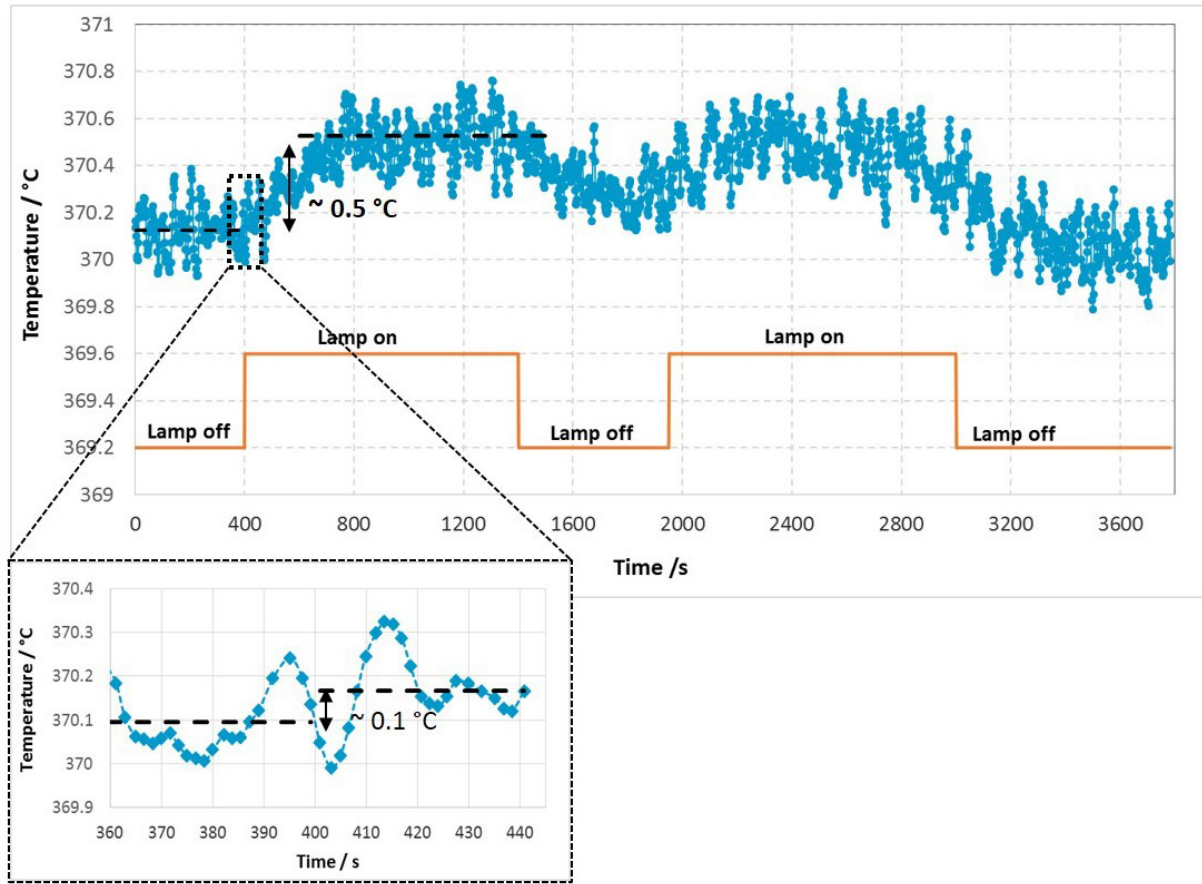


Figure 7. Phosphor response in the presence of strong IR background radiation.

Table 2. Uncertainty budget of phosphor thermometry in a field application at about 400 °C.

Uncertainty source	Standard uncertainty	Probability distribution function	Sensitivity coefficient	Uncertainty contribution (°C)
Phosphor calibration (u_{Cal})	0.336 °C	Normal	1	0.336
Repeatability of the lifetime estimate (u_{LTstd})	2.5 μs	Normal	$0.111 \text{ °C } \mu\text{s}^{-1}$	0.277
Exponential fitting residuals (u_{LTfit})	0.017 μs	Normal	$0.111 \text{ °C } \mu\text{s}^{-1}$	0.002
Data acquisition, sampling effect (u_{LTdaq})	0.086 μs	Normal	$0.111 \text{ °C } \mu\text{s}^{-1}$	0.01
Reproducibility of the phosphor coating method (u_{Repr})	3.5 μs	Normal	$0.111 \text{ °C } \mu\text{s}^{-1}$	0.389
Measurement standard uncertainty, u				0.58
Expanded uncertainty, $U = ku$ ($k = 2$)				1.16

($\text{Mg}_4\text{FGeO}_6\text{:Mn}$). The thermocouple was inserted into the aluminium billet along its entire length so that its sensitive tip was within 2 mm of the face of the billet on which phosphorescence and radiation measurements were performed.

The billet was placed in a horizontal Carbolite furnace (model TZF 13/38) and a suitable cold plate was set on the opening of the furnace in order to reduce the size-of-source effect error of the radiation thermometer (see figure 8). Once temperature stability of the furnace had been attained, simultaneous measurements with the three techniques were performed and compared. Figure 9 shows an example of the results of the three measurements near 380 °C. The measurement uncertainty bars represent the calculated expanded uncertainty, U , with a coverage factor $k = 2$, corresponding to

a coverage interval of about 95% [27]. The measurements are in agreement within the uncertainty, as can be seen from the graph and the summary in table 3.

3.2. Measurements in dynamic conditions

Measurements were also performed using the setup described above in dynamic conditions, i.e. during extraction of the aluminium billet from the furnace, thus simulating the typical cooling curve to which a billet sample is subjected as it leaves the industrial pre-heating furnace and is grabbed by a manipulation claw before being forged (see figure 10). The key parameter for ensuring good quality of the final product is the temperature of the billet when it leaves the furnace and

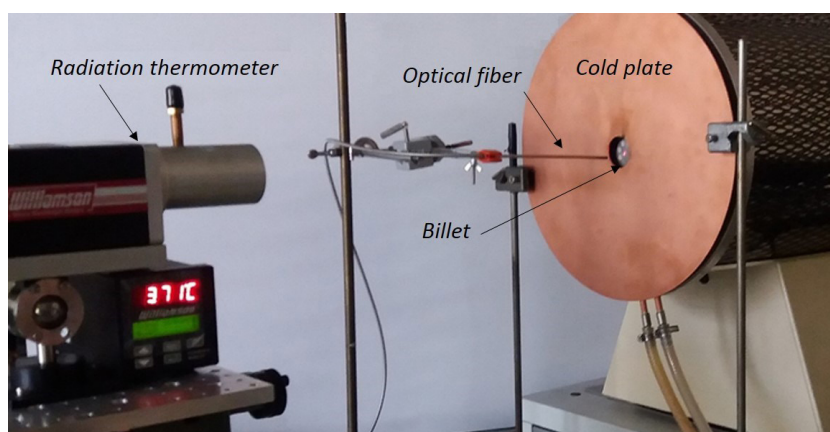


Figure 8. Arrangement for the measurements of the surface temperature of the billet with different techniques at the industrial manufacturing premises of Gamma Forgiati.

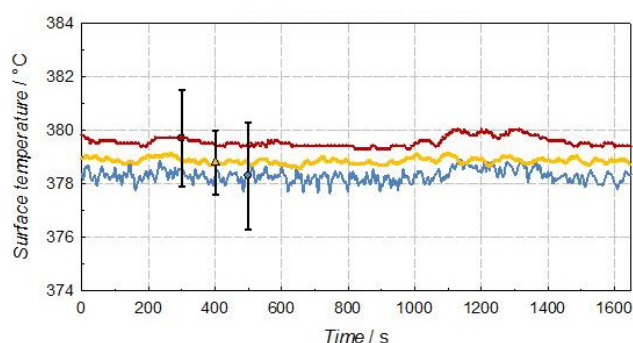


Figure 9. Surface temperature of the billet in stationary conditions: blue, IR radiation thermometer; yellow, phosphor-based thermometer; red, type-K thermocouple.

Table 3. Average values of the surface temperature of the billet as measured by the phosphor thermometer, the radiation thermometer and the type K-thermocouple with associated expanded uncertainties, U ($k = 2$).

Measurement technique	Surface temperature (°C)	Expanded uncertainty, U (°C)
Phosphor thermometer	378.8	1.2
Radiation thermometer	378.2	2.0
Type-K thermocouple	379.5	2.0

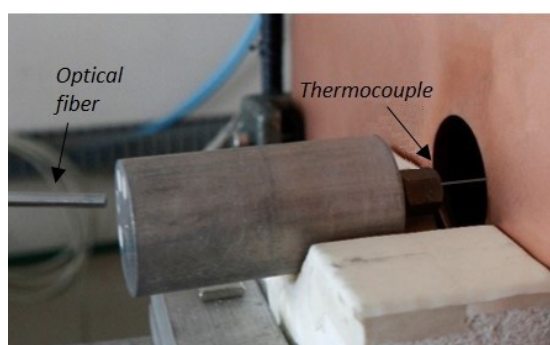


Figure 10. Aluminium billet during extraction from the horizontal furnace.

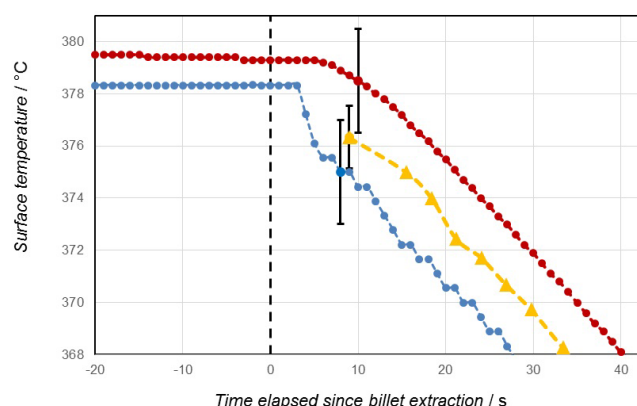


Figure 11. Surface temperature of the billet leaving the furnace as measured by the MW radiation thermometer (blue line), the phosphor-based thermometer (yellow line) and a type-K thermocouple (red line).

the lag time allowed before forging. Figure 11 gives the surface temperature during billet extraction. No data are available for the phosphor thermometer in the first seconds due to the time required for the positioning of the fibre in front of the phosphor spot. As can be seen from this diagram, all measurement results are consistent within their uncertainties, thus indicating a fairly good agreement between the three methods. The temperature evolution, as monitored over the course of several minutes after extraction, showed the same agreement as depicted in figure 11.

4. Conclusions

In the present work, a metrological validation of lifetime-based phosphor thermometry for industrial surface temperature measurements is presented. A dedicated fibre-optic phosphor-based thermometer for remote surface temperature measurements over the range from ambient to 450 °C was developed. The phosphor selected as a temperature-sensing material, $\text{Mg}_4\text{FGeO}_6\text{:Mn}$, was subjected to traceable calibration over

the whole temperature range and a dedicated electro-optical unit for the excitation and detection of its phosphorescence lifetime was developed. The performance of the thermometer was assessed and an analysis of the calibration uncertainty carried out. The phosphor-based technique was further validated by using a metal phase transition method: a spot of indium, which has a well-known melting temperature, was deposited on the surface of the calibration block with phosphor spots superimposed on it and the phosphorescence lifetime was then measured during the indium melting plateau. The thermometer was also tested in the presence of a strong IR background, in view of the IR likely to be present in field applications, and its measurement uncertainty was further assessed, thus resulting in an expanded uncertainty ($k = 2$) from 0.3 °C at room temperature up to less than 1.4 °C at 450 °C.

The phosphor thermometer was used in a case study at the industrial plants of Gamma Forgiati for surface temperature measurements of aluminium alloy billets during pre-heating before hot forging. In such a field application the phosphor-based technique was compared against an IR radiation thermometer and a contact thermometer. The experimental results showed that phosphor-based thermometry is a potential alternative approach to conventional methods. In addition, while giving results which are consistent with more traditional techniques, it potentially offers improved performance in terms of measurement uncertainty in the field. Despite the fact that the process of phosphor spot deposition makes this method less practical than radiation thermometry for on-line measurements in industry, it can be used to tune a manufacturing process off-line and, at the same time, provide measurement traceability through periodic *in situ* calibrations.

Acknowledgments

The work presented in this paper was performed in the framework of the EMPIR 14IND04 EMPRESS Project ‘Enhancing process efficiency through improved temperature measurement’. This project has received funding from the EMPIR programme co-financed by the Participating States and from the European Union’s Horizon 2020 research and innovation programme.

ORCID iDs

Lucia Rosso  <https://orcid.org/0000-0002-0633-8294>

Giulio Beltramino  <https://orcid.org/0000-0003-2058-3453>

References

- [1] Childs P R N, Greenwood J R and Long C A 2000 Review of temperature measurement *Rev. Sci. Instrum.* **71** 2959–78
- [2] Lempereur C, Andral R and Prudhomme J 2008 Surface temperature measurement on engine components by means of irreversible thermal coatings *Meas. Sci. Technol.* **19** 2959–78
- [3] Allison S W, Goedeke S, Beshears D, Cates M, Hollerman W, Womack F, Bergeron N, Bencic T, Mercer C and Eldridge J I 2003 Advances in high temperature phosphor thermometry for aerospace applications *39th AIAA/ASME/SAE/ASEE Joint Propulsion Conf. and Exhibition* (<https://doi.org/10.2514/6.2003-4584>)
- [4] Seyfried H, Richter M, Aldén M and Schmidt H 2007 Laser-induced phosphorescence for surface thermometry in the afterburner of an aircraft engine *AIAA J.* **45** 2966–71
- [5] Särner G, Richter M and Aldén M 2008 Investigations of blue emitting phosphors for thermometry *Meas. Sci. Technol.* **19** 125304
- [6] Eldridge J I, Allison S W, Jenkins T P, Gollub S, Hall C and Walker G 2016 Surface temperature measurements from a stator vane doublet in a turbine afterburner flame using a YAG:Tm thermographic phosphor *Meas. Sci. Technol.* **27** 125205
- [7] Fuhrmann N, Kissel T, Dreizler A and Brübach J 2011 Gd₃Ga₅O₁₂:Cr—a phosphor for two-dimensional thermometry in internal combustion engines *Meas. Sci. Technol.* **22** 045301
- [8] Zhao H 2007 *HCCI and CAI Engines for the Automotive Industry* (Cambridge: Woodhead Publishing) pp 498–500
- [9] Nada A, Fahd J, Hult J, Knappe C, Richter M, Mayer S and Aldén M 2014 A first application of thermographic phosphors in a marine two-stroke diesel engine for surface temperature measurement *Proc. of the ASME 2014 Internal Combustion Engine Division (ICEF2014)* (<https://doi.org/10.1115/ICEF2014-5417>)
- [10] Nemitz W, Fulmek P, Nicolics J, Reil F and Wenzl F P 2017 On the determination of the temperature distribution within the color conversion elements of phosphor converted LEDs *Sci. Rep.* **7** 9964
- [11] Cao Y, Koutsourakis G, Sutton G, Kneller J, Wood S, James B and Castro F 2019 *In situ* contactless thermal characterization and imaging of encapsulated photovoltaic devices using phosphor thermometry *Prog. Photovolt. Res. Appl.* **27** 673–81
- [12] Cates M R, Beshears D L, Allison S W and Simmons C M 1997 Phosphor thermometry at cryogenic temperatures *Rev. Sci. Instrum.* **68** 2412–7
- [13] Cates M, Allison S W, Jaiswal S and Beshears D 2003 YAG:Dy and YAG:Tm phosphorescence to 1700 °C *Proc. of the ISA’s 49th Int. Instrumentation Symp.* vol 49 pp 389–400
- [14] Fuhrmann N, Brübach J and Dreizler A 2013 Phosphor thermometry: a comparison of the luminescence lifetime and the intensity ratio approach *Proc. Combust. Inst.* **34** 3611–8
- [15] Allison S and Gillies G 1997 Remote thermography with thermographic phosphors: instrumentation and applications *Rev. Sci. Instrum.* **68** 2615–50
- [16] Khalid A and Kontis K 2008 Thermographic phosphors for high temperature measurements: principles, current state of the art and recent applications *Sensors* **8** 5673–744
- [17] Chambers M D and Clarke D R 2009 Doped oxides for high-temperature luminescence and lifetime thermometry *Annu. Rev. Mater. Res.* **39** 325–59
- [18] Aldén M, Omrane A, Richter M and Särner G 2010 Thermographic phosphors for thermometry: a survey of combustion applications *Prog. Energy Combust.* **37** 422–61
- [19] Brübach J, Pflitsch C, Dreizler A and Atakan B 2013 On surface temperature measurements with thermographic phosphors: a review *Prog. Energy Combust. Sci.* **39** 37–60
- [20] Yi S J and Kim K C 2014 Phosphorescence-based multiphysics visualization: a review *J. Vis.* **17** 253–73
- [21] Everest M and Atkinson D 2008 Discrete sums for the rapid determination of exponential decay constants *Rev. Sci. Instrum.* **79** 023108
- [22] Brübach J, Feist J and Dreizler A 2008 Characterization of manganese-activated magnesium fluorogermanate with

- regards to thermographic phosphor thermometry *Meas. Sci. Technol.* **19** 025602
- [23] Wickersheim K and Sun M 1987 Fiberoptic thermometry and its applications *J. Microwave Power* **22** 85–94
- [24] Webster T and Cunningham G 2000 Design, manufacturing and testing of a boiler metal surface temperature probe *Proc. 2000 Int. Joint Power Generation Conf.* p 1370
- [25] Omrane A, Ossler F and Aldén M 2002 Two-dimensional surface temperature measurements of burning materials *Proc. Combust. Inst.* **29** 2653–9
- [26] Brübach J, Patt A and Dreizler A 2006 Spray thermometry using thermographic phosphors *Appl. Phys. B* **83** 499–502
- [27] BIPM, IEC, IFCC, ILAC, ISO, IUPAC, IUPAP and OIML 2008 Evaluation of measurement data *Guide to the Expression of Uncertainty in Measurement* (Joint Committee for Guides in Metrology, JCGM 100)
- [28] Ding R, Zhao M J, Cabana D and Chen D 2008 Comparison between melting and freezing points of indium and zinc *NCSLI Meas.* **3** 70–4